JGR Earth Surface

RESEARCH ARTICLE
10.1029/2019JF005273

Quantification of Peat Thickness and Stored Carbon at the Landscape Scale in Tropical Peatlands: A Comparison of Airborne Geophysics and an Empirical Topographic Method

Sonia Silvestri[1,2], Rosemary Knight[3], Andrea Viezzoli[4], Curtis J. Richardson[2], Gusti Z. Anshari[5], Noah Dewar[3], Neal Flanagan[2], and Xavier Comas[6]

[1]Department of Biological, Geological, and Environmental Sciences, University of Bologna, Bologna, Italy, [2]Nicholas School of the Environment, Duke University, Durham, NC, [3]School of Earth, Energy and Environmental Sciences, Stanford University, Stanford, CA, [4]Aarhus Geophysics, Aarhus, Denmark, [5]Tanjungpura University, Pontianak, Indonesia, [6]Department of Geosciences, Florida Atlantic University, Boca Raton, FL

Abstract Peatlands play a key role in the global carbon cycle, sequestering and releasing large amounts of carbon. Despite their importance, a reliable method for the quantification of peatland thickness and volume is still missing, particularly for peat deposits located in the tropics given their limited accessibility, and for scales of measurement representative of peatland environments (i.e., of hundreds of km^2). This limitation also prevents the accurate quantification of the stored carbon as well as future greenhouse gas emissions due to ongoing peat degradation. Here we present the results obtained using the airborne electromagnetic (AEM) method, a geophysical surveying tool, for peat thickness detection at the landscape scale. Based on a large amount of data collected on an Indonesian peatland, our results show that the AEM method provides a reliable and accurate 3-D model of peatlands, allowing the quantification of their volume and carbon storage. A comparison with the often used empirical topographic approach, which is based on an assumed correlation between peat thickness and surface topography, revealed larger errors across the landscape associated with the empirical approach than the AEM method when predicting the peat thickness. As a result, the AEM method provides higher estimates (22%) of organic carbon pools than the empirical method. We show how in our case study the empirical method tends to underestimate the peat thickness due to its inability to accurately detect the large variability in the elevation of the peat/mineral substrate interface, which is better quantified by the AEM method.

Plain Language Summary Peatlands store in their soils about the same amount of carbon present in the vegetation biomass. Peat degradation due to human interventions (as for example soil drainage) and fires that occur during severe droughts release several gigatons of carbon dioxide and other greenhouse gases (GHGs) every year. The accurate assessment of the carbon stored in peatlands is of key importance to implement effective strategies to mitigate climate change, promoting conservation actions, and avoiding potential GHG emissions. In this research, we compare two methods that allow us to construct a 3-D model of peatlands. Applying the methods to a large study site in Indonesia, we show how a geophysical method called airborne electromagnetics allows for a more accurate quantification of the peat volume and the organic carbon pool.

Key Points:
- The airborne electromagnetic (AEM) method can detect both the top and the bottom of a peatland over large areas at high spatial resolution
- A correlation between the peat thickness and surface topography is common in some dome-shaped peatlands around the world
- The peatland 3-D model retrieved with AEM is superior if compared to the empirical approach that links peat thickness to only soil elevation

Supporting Information:
- Supporting Information S1
- Figure S1
- Figure S2
- Figure S3
- Figure S4
- Figure S5
- Figure S6

Correspondence to:
S. Silvestri,
sonia.silvestri@duke.edu

Citation:
Silvestri, S., Knight, R., Viezzoli, A., Richardson, C., Anshari, G. Z., Dewar, N., et al. (2019). Quantification of peat thickness and stored carbon at the landscape scale in tropical peatlands: A comparison of airborne geophysics and an empirical topographic method. *Journal of Geophysical Research: Earth Surface*, *124*. https://doi.org/10.1029/2019JF005273

Received 22 JUL 2019
Accepted 10 DEC 2019
Accepted article online 14 DEC 2019

1. Introduction

Global estimates report that peatlands store in their soils about the same amount of carbon stored in the world's vegetation phytomass (i.e. sum of the aboveground and the belowground biomass), with values that range between 400 and 600 Pg depending on authors (Scharlemann et al., 2014; Yu et al., 2010; Gorham, 1991). The uncertainty in these estimates is mainly due to our inability to accurately quantify the volume of peat found in peatlands, an accurate estimation of which is needed to determine the amount of stored carbon (Page et al., 2002; Ballhorn et al. 2009; Turetsky et al., 2015; Warren et al., 2017). Ground-based studies can use coring, probing, and geophysical methods to estimate peat volume in small peatlands or portions of them but cannot provide the spatial coverage needed to obtain estimates of stored carbon over larger areas.

In order to estimate the volume of a peatland, the simultaneous quantification of its areal extent, topographic elevation, and bottom morphology and depth are needed.

The surface morphology of peatlands, especially those with domed surfaces, has long fascinated ecologists, geomorphologists, and remote-sensing experts. The topography of peatlands, their development over time, and their dependence on hydrological variables, i.e., rainfall and drainage patterns, have been studied extensively in the past (Ingram, 1982; Clymo, 1984; Foster & Wright, 1990; Belyea & Baird, 2006). Thanks to these efforts, we know that the topographic shape and patterns within peatlands reflect the interactions between the underlying terrain form, vegetation, climate, and hydrology (Rydin & Jeglum, 2013). Much effort has also been devoted to inferring peatland morphology using airborne and satellite sensors in order to describe their areal extent (Ballhorn et al., 2011; Dargie et al., 2017; Miettinen et al., 2012) and surface elevation (Draper et al., 2014; Jaenicke et al., 2008) including possible changes in topographic elevation related to peat degradation (Ballhorn et al., 2009). However, even though past efforts have traditionally focused on the characterization of the surface morphology of peatlands, e.g., its topography and extent, the importance of the morphology of the peat bottom has been understudied. Previous studies have demonstrated the ability of certain ground-based geophysical methods such as ground-penetrating radar or electrical resistivity imaging to characterize the morphology of the peat/mineral-soil interface (Slater & Reeve, 2002; Comas et al., 2015; Parsekian et al., 2011), and ultimately to use these measurements to infer carbon stocks in peatlands (Comas et al., 2017; McClellan et al., 2017). However, these measurements are typically limited by their scale of measurement since they require direct contact with the ground surface.

In this work, we use a novel remote geophysical approach based on very high spatial resolution measurements acquired using the airborne electromagnetic (AEM) method to detect the bottom of the peat profile of a large Indonesian mire and consequently quantify its volume and infer total stored carbon at the landscape (km) scale. The AEM method that we applied utilizes the contrast in electrical resistivity between the peat and the underlying substrate thus allowing for the detection of the bottom surface of the peatland. The success in the application of this approach depends on the specific characteristics of the instrument used for the survey as well as on the electrical resistivity contrast between the peat and the substrate. Moreover, since peatlands may also be formed by very thin peat layers, the ability of this geophysical method to detect and resolve very near surface structures was also assessed.

In order to determine the accuracy of the 3-D model of the peatland retrieved using the AEM method we used two approaches, i.e., (a) the validation of the peat thicknesses at specific locations using a large dataset of field point measurements and (b) the quantitative comparison of the AEM 3-D model with a 3-D model created using a more traditional approach based on an empirical correlation between peat thickness and peatland surface topography.

The empirical approach used here for comparison comes from recent studies (Deltares, 2016; Rudiyanto et al., 2015; Hooijer & Vernimmen, 2013; Parry et al., 2012; Holden & Connolly, 2011; Jaenicke et al., 2008) that have suggested the presence of a correlation between peat thickness and peatland surface elevation mainly for Asian peatlands. Such a correlation, if properly established, would allow the quantification of the peat volume by simply retrieving the topography of the peatland surface (using for example LiDAR surveys, e.g., Deltares, 2016). As often happens with empirical approaches, the success in the application of such methodology raises three main research questions: (1) How general is the existence of a correlation between peat thickness and surface elevation across the world's peatlands? (2) Once a correlation is found in one area, how transferable is it to other areas as the basis for inferring peat thickness? (3) If given a positive answer to (1) and (2), can one, with confidence, adopt the use of a correlation between thickness and elevation as a method to accurately quantify peat volume at the local, regional, and landscape scale? In this work we address these questions and then compare the accuracy of the 3-D model extracted from AEM data to the model produced using the apparent correlation of peat thickness to surface topography.

2. Methods

2.1. Study Site and Data Acquisition

The site selected for this study covers an area of approximately 23,500 ha in West Kalimantan, Indonesia (Figure 1). It is delimited to the north by the Kapuas River, which in this tract forms three large

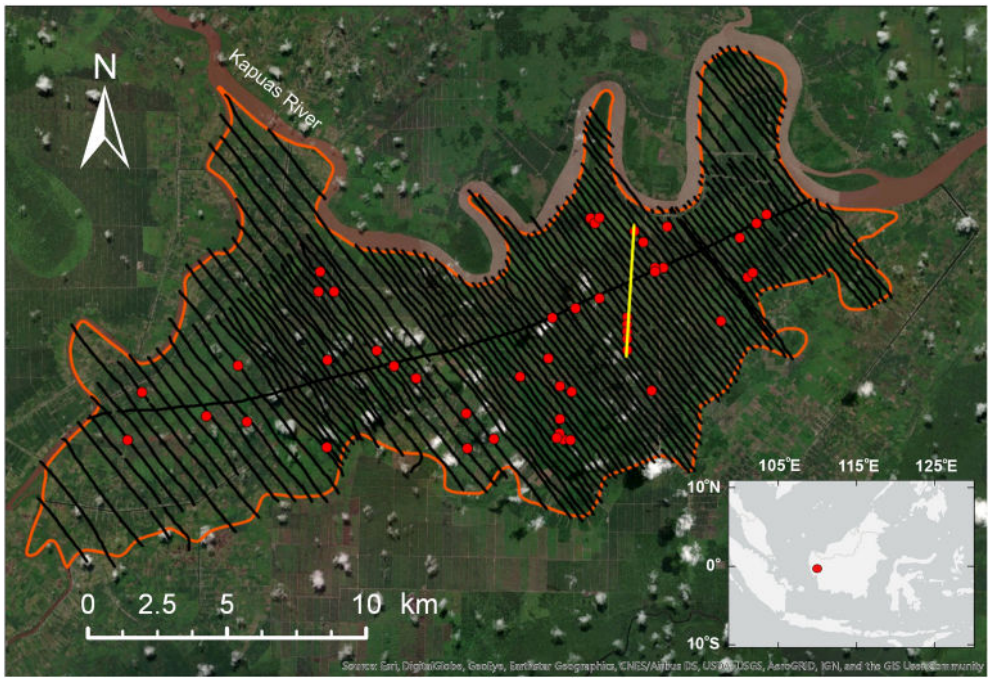

Figure 1. Study site located in Kubu Raya District, West Kalimantan, Indonesia. Red dots indicate the field measurement sites; AEM flight lines are plotted in black; the yellow line shows the location of the transect of Figure 2 (created using ESRI ArcGIS – DigitalGlobe, GeoEye, Earthstar Geographics, CNES/Airbus DS, USDA, USGS, AeroGRID, IGN, and the GIS User Community).

meanders, and to the south by agriculture land. The study site is now almost entirely covered by agriculture land and villages, but before deforestation, the majority of the territory was covered by dense forests until early 1990. The study site includes two different raised mires, the largest is located in the East part of the site while the one located in the West part is smaller. The difference between the two mires may be due to the fact that the deforestation started about 30 years ago in the West part of the study site, while the East side remained forested until recently.

2.1.1. Field Measurements and Laboratory Analyses

Field-based estimates of peat thickness were collected using soil coring equipment at a total of 63 locations across the study area (Figure 1). Core locations were selected to represent a range of peat depths and geomorphic settings and were at least 10 m away from established foot paths in areas with minimal disturbance of existing plant ground-cover. Geographic positions were recorded with a handheld GPS (Ashtech Promark 100) with horizontal error of less than 1 m. Cores were obtained with a Russian-style peat corer (Eijkelkamp Agrisearch Equipment), which collects a semiundisturbed core, a half-cylinder 5 cm in diameter, at 50-cm depth increments. During coring the physical properties of the peat profile and underlying mineral soils (clay, loam, silt, and sand) were evaluated and recorded. Peat is defined as a material that has accumulated in situ and consists of at least 30% (dry mass) of dead organic material (Joosten et al., 2017) and is taxonomically described as a soil found in the order Histosol, which primarily consists of partially decomposed organic matter that has accumulated in a horizon at least 40-cm thick with a minimum organic carbon content of between 12 and 18% depending on the clay content (FAO, 1988; FAO, 1998; Soil Survey Staff, 2014a). Within each depth increment, peat material was inspected for degree of decomposition using the Von Post Method (Von Post & Granlund, 1926) and for indicators of increasing mineral content (sand, silt, and clay) using color, soil ribbon techniques, and soil plasticity tests (Soil Survey Staff, 2014b). The boundary between peat and the underlying mineral sediments was established using USDA (United States Department of Agriculture) criteria to classify soil into predominantly peat or mineral categories (Soil Survey Staff, 2014a). The deepest core increment typically contained the peat/mineral-soil boundary with peat near the top and mineral soil near the bottom of the sample-chamber. Soil subsamples were collected from each depth increment at 18 coring locations, weighed in the field, labeled, and packaged using aluminum foil, half PVC storage, and polyethylene wrap. Samples were transported to laboratory facilities at Tanjungpura

University where analyses of soil moisture content, bulk density, and specific conductance (described below) were performed according to standard methods. Moisture contents were measured by drying samples at 70 °C in the oven until a constant weight, and contents of organic matters were measured by combusting 2–3 g of dried samples at 550 °C (Anshari et al., 2010; Könönen et al., 2015). These values were used to determine the amount of soil organic matter and the organic carbon content by soil volume.

The spatial variability of peat thickness at this study site was determined based on 11 of the locations visited in late November 2017. At each one of these locations, one point was selected for sampling the full core depth while two additional cores were arranged in a triangular pattern with the vertices (cores) spaced between 0.5 and 6 m apart (with one single triplet that contains one core ~11 m from the other two). The two nearby cores were acquired to sample the base of the peat so as to determine peat depth and an estimate of its local spatial variability; this provided 22 additional measurements of peat thickness.

During the field campaigns, while the locations were determined using GPS, the measured surface elevations were not recorded due to the low vertical precision of the instrument and the limited time available for the surveys. In order to assign the surface elevation to the core locations, we used the digital elevation model produced through the interpolation of the SkyTEM altimeter data (see section 2.1.3 for details).

2.1.2. Electrical Resistivity Measurements

Laboratory and field measurements of electrical resistivity were performed with the purpose of guiding us in separating peat from the underlying material in the AEM data analysis. Bulk electrical resistivity was recorded during core extraction at several depths within the peat column using a 5TE capacitance moisture probe from Decagon, which measures electrical resistivity using a stainless steel electrode array. At each primary coring location, electrical resistivity measurements were made approximately every 50 cm. When the material present in the core was visibly heterogeneous over the measurement interval of 50 cm, the measurements were increased to every 20 cm. If a clear boundary was visible between two materials in the measurement interval, additional measurements were then taken immediately above and below the boundary.

Electrical resistivity measurements were also made in the laboratory on 25 of the core samples collected in the field. Samples were prepared as mixtures of 10 g of solid and 10 ml of pure water. The samples were homogenized for 1 h, and then measured with a WTW Conductivity Meter 3210.

2.1.3. The Airborne Electromagnetic Method

The instrument selected for this study, SkyTEM, is a helicopter-deployed time domain EM system (Sørensen & Auken, 2004). This specific instrument was selected because of its high sensitivity to near surface strata due to its accurate early time returns (Schamper et al., 2014). The AEM method has been widely used for groundwater exploration and the mapping of groundwater systems (Høyer et al., 2015; Knight et al., 2018; Podgorski et al., 2013; Sattel & Kgotlhang, 2004). Its applicability for the detection of peatlands comes from recent advancements in the technology that have increased the ability to obtain measurements with high vertical resolution at shallow depths.

There are a number of parameters that can impact the applicability of AEM to peatland studies. We modeled numerous scenarios and found that the key parameters are the thickness of the peat and the contrast between the resistivity values of the peat and the substrate. The results of our feasibility analysis are included in the Supporting Information. We found that when the resistivity contrast is large, there is high ability to detect the change in resistivity at the bottom of the peat and accurately recover the peat thickness. The accuracy degrades as the peat thins or as the resistivity contrast decreases. As the resistivity contrast is decreased or becomes variable, the mapped depth of the bottom of the peat becomes more uncertain, and the accuracy of the estimate for the peat thickness is reduced. Whenever the peat and the substrate have the same resistivity value, the AEM method cannot determine the thickness of the peat. When the peat thickness is ~1 m or thinner, the resistivity contrast must be extremely large in order to allow an accurate thickness detection.

The SkyTEM system used in this study is a time-domain electromagnetic system carried as an external sling load below the helicopter. Current flows through a transmitter loop, setting up a magnetic field. This field generates eddy currents in the subsurface that generate a secondary magnetic field, the temporal variation of which is recorded by the receiver coils as the field data. The SkyTEM system was used in November 2017 to collect data on the study site. The system collects data along flight lines, i.e., continuous lines formed by returns that, near surface, have a footprint with a diameter of ~40 m. The distance between useful contiguous returns along the flight lines depends on the sampling rate, the speed of the helicopter, and the

signal to noise ratio. For this survey it averages about 30 m. The total length of the flight lines along which data were acquired was 827 km, covering an area of 23,524 ha (235 km^2). The distance between the 110 parallel flight lines was variable: most of the lines were separated by ~230 m; however, there are lines that were separated by ~460 m, and a few lines were separated by ~920 m. The helicopter carrying the system flew at an average speed of ~100–115 km/h, at an altitude of 25–65 m above the ground.

The acquired data were processed and inverted to obtain a model of the subsurface electrical resistivity of the region. Advanced processing was applied in order to prepare the data for the inversion. This includes data corrections and filtering, culling, and discarding of distorted or noise-affected data. The remaining data were then averaged spatially using trapezoid filters, which improves the signal to noise level without compromising lateral resolution. Data processing was carried out using the SkyTEM module of the Aarhus Workbench software package (Aarhus GeoSoftware, 2018).

Preliminary inversions were carried out using the quasi-2-D laterally constrained inversion (Auken & Christiansen, 2004). Final inversions were carried out using the quasi-3-D spatially constrained inversion (Viezzoli et al., 2008). Laterally constrained inversion and spatially constrained inversion are full nonlinear damped least squares solutions in which the transfer function of the instrumentation is modeled. This includes, among other things, current turn-on and -off ramps, front gate and low pass filters, system altitude, etc. The inversion kernel is "AarhusInv", designed by the University of Aarhus (Kirkegaard & Auken, 2014).

The inversion performed using 25 layers was chosen as the one that best described the spatial distribution of the peat.

In addition to the electromagnetic data, the SkyTEM system also provides independent data collected with two laser altimeters placed on the frame that measure the distance to the ground surface along the flight line. The tilt, roll, and yaw of the frame are measured with two inclinometers. After filtering out first returns and retaining only last returns along the flight lines, these data were used to produce a surface digital elevation model with an accuracy of ± 1 m (Sørensen & Auken, 2004).

In order to determine the surface and the bottom topography of the peatland from the SkyTEM data, we performed an interpolation of both the soil elevation detected by the altimeters and measurements of the bottom of the peat layer extracted from the resistivity model produced from the SkyTEM data via inversion. Several methods were tested, including spline interpolation, ordinary kriging, and Empirical Bayesian kriging with different fitting functions (performed in ArcGIS Pro), all performed on a grid with 40×40 m pixels (according to the footprint of the SkyTEM data). The method that gave the best results in terms of cross validation with the field measurements was the Empirical Bayesian kriging with a power semivariogram model.

2.1.4. Correlation Between Peat Thickness and Peatland Topography

In order to investigate the existence of a correlation between peat thickness and peatland topography we used data extracted from studies performed in North and South America, Europe, Africa, and Asia to carry out a comprehensive analysis examining commonalities and differences in both the surficial and bottom topography of peatlands from varied climatic conditions and at very different latitudes. Capturing the topo-stratigraphic profiles contained in several of these studies, we measured the surface elevation, and the peat thickness along the profiles at the points where coring was performed by the authors of the original study. The transects generally ran across the mire starting from a stream or river, reaching the center of the mire and eventually proceeding to the opposite side where there might be a second river (Esterle & Ferm, 1994; Page et al., 1999). The selected mires varied considerably in terms of morphology and included both domed peatlands and mires with other surface morphologies (e.g. flat, concave, or irregular). For each study, in order to address our first research question, we analyzed the relationship between peat thickness and surface elevation. The complete list of the original studies examined and the correlation parameters are reported in Table S1 (Supplementary Information).

The main error we expect from these older studies is due to the difficulty in measuring the absolute elevation above a certain level (e.g., mean sea level or the mean level of the nearest river). This difficulty was present in these older studies due to the unavailability/uncertainty of GPS systems or difficulties related to using topographic measurement techniques in remote areas. However, as we show in the Supporting Information, the absolute elevation does not affect the slope of the regression line between peat thickness and surface elevation thus having no impact on the accuracy of our model.

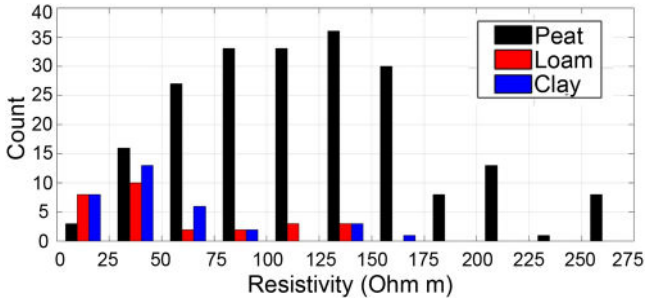

Figure 2. Distribution of the electrical resistivity measurements made in the field and in the laboratory on peat and the underlying material – described here as loam and clay.

Another possible source of error is related to the methodology used when collecting cores. The vast majority of the examined peatland studies measure the thickness of the peat using push probes or Russian peat corers (DeLaune et al., 2013) hence directly determining the thickness of the peat layer above the substratum. These measurements are point estimates of the peat thickness, and their success can be affected by the presence of pieces of wood or other materials that prevent the perforation and affect the accuracy of the measurements, especially when push probes are used (Parry et al., 2014). For this reason, some of the studies that we examined that are based on push probe measurements may have larger errors than those studies that used peat corers.

Ground-based geophysical methods, such as ground penetrating radar and electrical resistivity imaging, have been shown to be highly effective in detecting peat thickness at high spatial resolution (Comas et al., 2015; Slater & Reeve, 2002; Warner et al., 1990). Unfortunately, most of the geophysical studies we examined do not report the surface elevation, and thus, we could not use them in this study to correlate peat thickness and surface topography.

At our study site, the empirical model was calculated separately for the West and East mires using the peat thickness measured in the field and the corresponding surface elevations extracted from the digital elevation model. The accuracy of the empirical model in predicting the peat thickness was calculated using a variant of K-fold cross validation, i.e., dividing the data set into test and training sets and averaging the mean squared error (MSE) across all trials. For the West mire, we always used a test set of 5 points for validation and training sets of 5, 7, and 9 points for calibration. For the East mire, given the much larger data set available, we used a test set of 14 points for validation and training sets of 4, 5, 7, 10, 15, 20, 25, 30, and 35 points for calibration. Moreover, we also considered the whole dataset of 63 field measurements with a test set (for validation) of 14 points and training sets (for calibration) of 4, 5, 7, 10, 15, 20, 25, 30, and 35 points.

3. Results

3.1. Electrical Resistivity of Peat and Substrate

The distribution of electrical resistivity measurements performed in the field and in the laboratory is reported in Figure 2. From the figure, we see that when the resistivity values fall below 25 Ohm-m, there is an increased probability that resistivity value corresponds to the presence of mostly substrate material – here described as clay and loam. There were a few peat samples with very high values of electrical resistivity; they are omitted in this figure so as to more clearly display the measurements at in the lower part of the resistivity range. As can be seen in this figure, the resistivity of the peat varies over the entire range of measured values for all three materials. This implies that it would be challenging, in some cases, to differentiate peat from the substrate material based on electrical resistivity values alone. In the resistivity interval 25–50 Ohm-m, the number of peat measurements is considerably lower than for values larger than 50 Ohm-m. Based on these observations, we selected as an initial estimate a conservative resistivity threshold between peat and the underlying material of ~50 Ohm-m. This was later refined through a more comprehensive interpretation of the subsurface resistivity structure of the study site performed by examining the spatial distribution of resistivity retrieved from the AEM data (see paragraph 3.2).

3.2. Peat Thickness from the Airborne Electromagnetic Method

The profile relative to the yellow transect included in Figure 1 is visible in Figure 3, where blue colors are assigned to resistivities lower than 20 Ohm-m, greens are assigned to the interval 20–35 ohm-m, yellows to the 35–55 Ohm-m interval, and finally the orange-reds indicate resistivities higher than 55 Ohm-m. Based on this and other transects that show the fast vertical variability shift for resistivity interpreted as corresponding to the transition between peat and the substrate, and also considering the resistivity distribution measured in the field/lab (Figure 2), 45 Ohm-m was chosen as threshold for the interface between the peat and the underlying clay. We note that the 45 Ohm-m value also well describes the results obtained from coring (Figure 3).

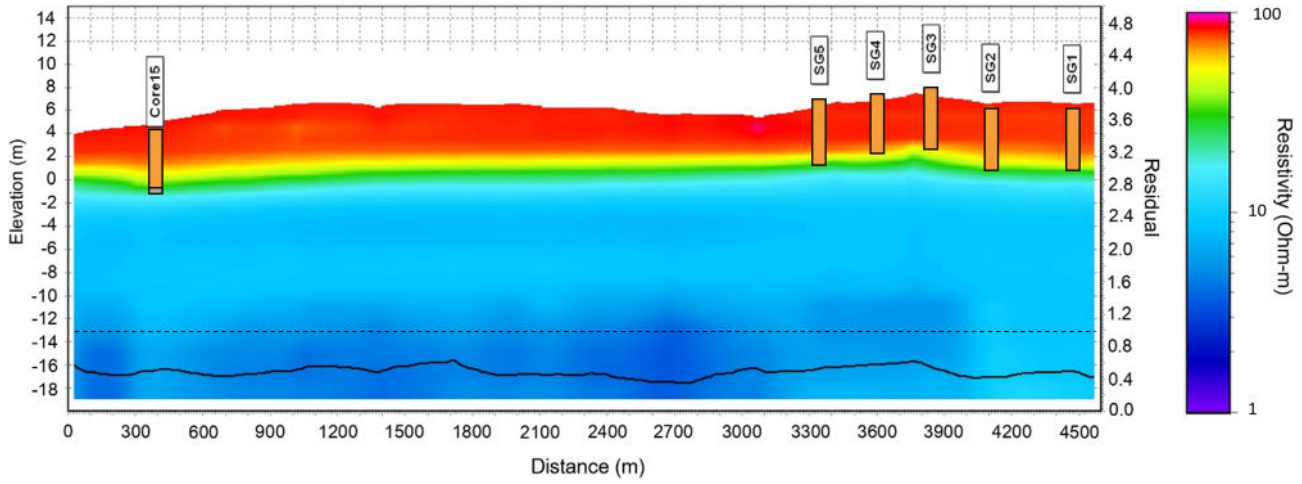

Figure 3. AEM resistivity model retrieved for the yellow transect of Figure 1 and compared with soil profiles from coring. Legend of the corings: Orange = Peat; Gray = Mineral substrate (Clay). The continuous black line at the bottom represents the data misfit (to be read against the right axis). The dash line shows Misfit 1, below which modeled data fit measured data.

Once the 45 Ohm-m resistivity threshold was chosen, we could create a 3-D model of the peatland. Figure 4a shows the map of the peat thickness distributed across the study site, where the 63 field measurements are superimposed using the same color-coded palette used for the map. We notice that, as originally speculated, there are two juxtaposed mires within the site, one in the West and one in the East portion of the area. The East dome is much larger than the West dome, with peat thicknesses higher than 6 m. Its shape is more regular and almost entirely covers the East half of the study site. The West mire covers only the center of the West portion of the study site.

The overall accuracy of the AEM method in detecting the peat thickness along the flight lines is visible in Figure 4b where we plot the thickness retrieved from the AEM data versus the thickness measured in the field at the 14 locations where the distance between the AEM measurement locations and the nearest field measurement is less than 20 m. Such a distance was selected because, as already mentioned, the SkyTEM data have a measurement footprint with diameter of ~40 m. The regression shows that the AEM method

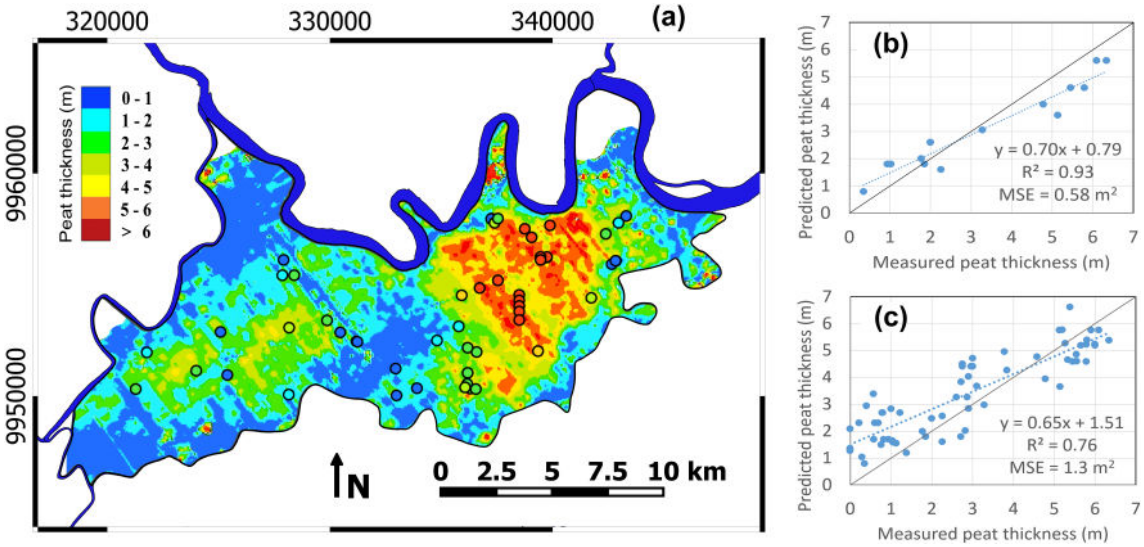

Figure 4. (a) Peat thickness map of the study site obtained with the AEM method with field measurements superimposed (same color-coded palette). The two panels to the right show the scatter plots of predicted versus measured peat thickness values performed using the AEM method, with (b) the 14 field measurements falling within a distance of 20 m from the SkyTEM returns, (c) all the 63 available field measurements. MSE = mean squared error.

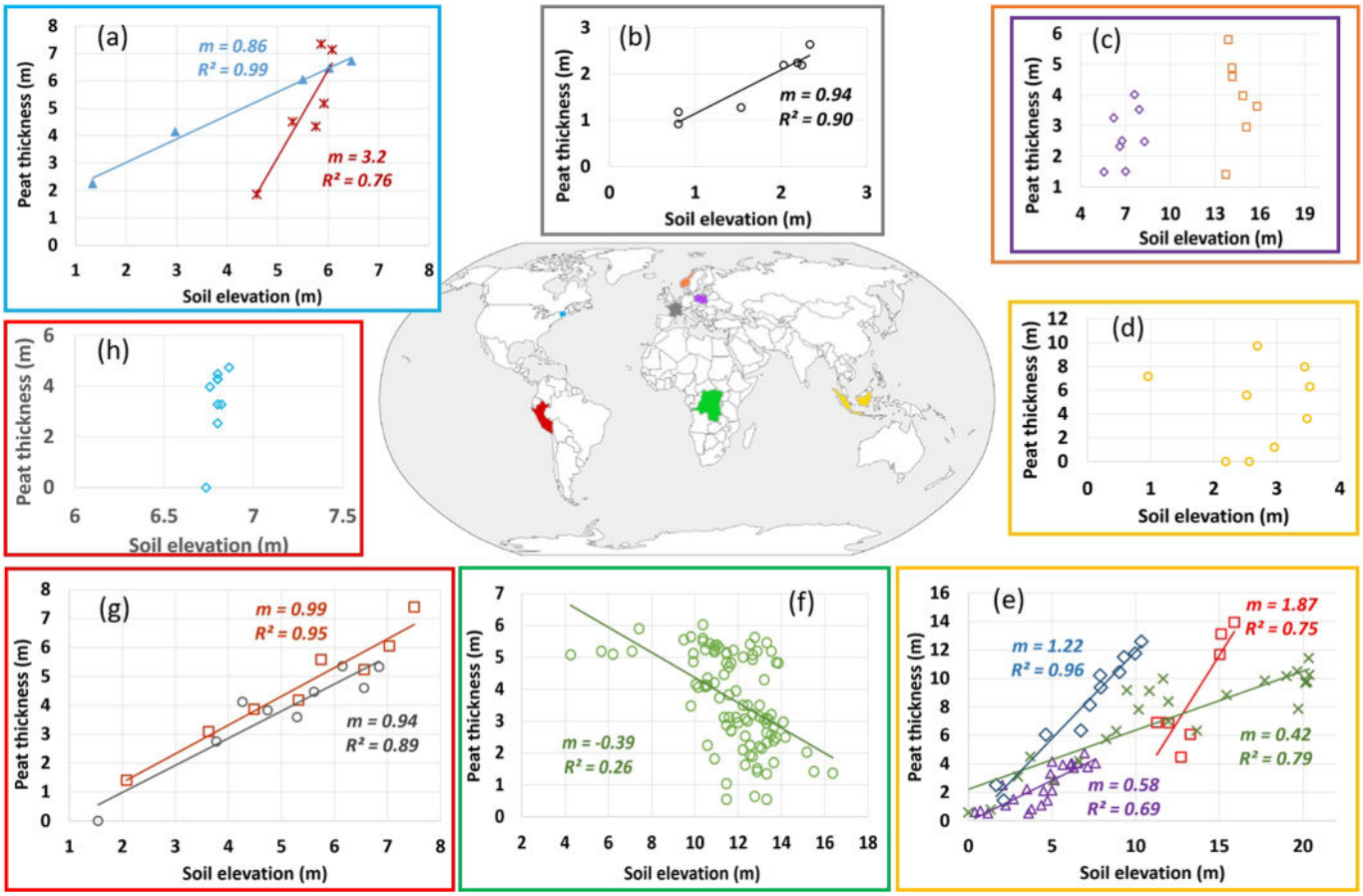

Figure 5. Correlations between peat thickness and soil surface elevation extracted from studies that report measurements recorded in locations situated in Asia, Africa, Europe, South, and North America. Data are extracted from the following sources: (a) – Cameron and Schruben (1983) (dark red crosses: first bog to the left of "their figure 2", points 49-5; blue triangles: third bog from the left of "their figure 2" points 68-16 – Maine, USA); (b) – Cubizolle et al. (2007) (France); (c) – Kowalczyk et al. (2017) (purple circles – Poland) and Silvestri et al. (2019) (orange squares – Norway); (d) – Esterle and Ferm (1994) ("their figure 5" – yellow circles – Indonesia); (e) – Esterle and Ferm (1994) ("their figure 4" – blue diamonds – Indonesia), Supardi and Neuzil (1993) ("their figure 8" – red squares – Indonesia), Page et al. (1999) (green crosses – Indonesia), Anshari, personal communication (purple triangles – Indonesia); (f) – Dargie et al. (2017) (Congo); (g) – Lähteenoja and Page (2011) – ("their Figure 3a" – dark red squares – Peru and "their Figure 3b" – gray circles – Peru); (h) – Lähteenoja and Page (2011) ("their Figure 3d" – Peru). The elevation is referred to a different zero for each data set, e.g., referred to the mean sea level or to another local reference as specified in the supporting information.

performs very well, with mean squared error of 0.6 m^2. In general, we note that the method slightly overestimates the peat thickness where it is very shallow (less than 1 m) and underestimates it where it is thicker than 5 m. The bias can be corrected using a small number of field measurements; however, we decided not to perform the correction in order to demonstrate the accuracy of the AEM method with no constrains.

The overall accuracy of thickness predicted with the AEM method decreases when we compare the peat thickness measured at all of the 63 points (including those farther than 20 m) with the thickness interpolated from the AEM data (Figure 4c). In this case, the MSE equals 1.3 m^2. This indicates that the thickness estimated by interpolation of the AEM data at the field points is affected by larger errors. This is probably due to the high spatial variability of the peat thickness that we have observed in the field; this is discussed in the Supporting Information (see also Figure S5 of the Supporting Information).

3.3. The Empirical Topographic Approach

Our analysis of previous studies found that a linear correlation between peat thickness and surface elevation is very common in many domed peatlands. Figure 5 shows several examples (only regression lines with *p*-value lower that 0.05 are shown). Looking at the regression lines in Figures 5a, 5b, 5e, and 5g, we find that the slope *m* varies considerably from case to case, with values that can be close to 0 (e.g.. $m = 0.42$, Page et al., 1999) or greater than 3 (e.g. $m = 3.2$, Cameron & Schruben, 1983).

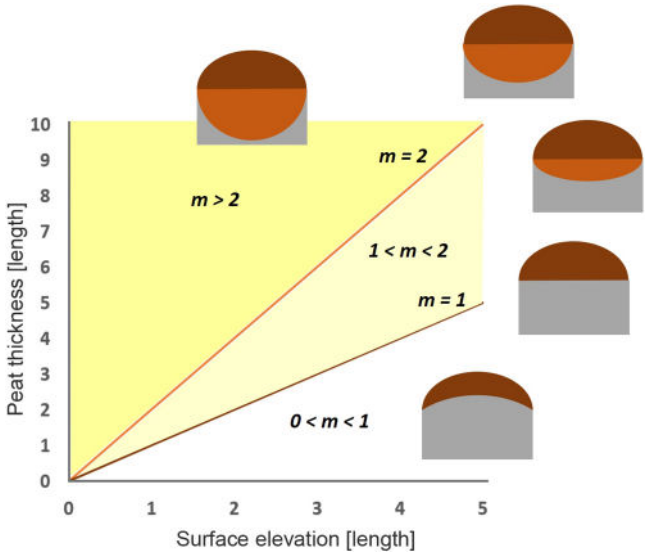

Figure 6. Simplified peatland morphologies corresponding to different values of the slope *m*.

The linearity of the relationship between peat thickness and surface elevation is not trivial; it implies that, along the measuring transects, the bottom profile of the peat mires covaries with the topography (see also Figures S1a–S1c on the Supporting Information). The observed behavior also implies that the highest elevation point of the top of the mire corresponds to the lowest elevation point of the bottom of the mire when the top surface is convex and the bottom surface concave and to the highest elevation point of the bottom surface when both surfaces are convex. In cases such as these, measurements of surface topography could be used to estimate peat thickness if the value of *m* was known.

Despite the numerous examples of a linear correlation between thickness and elevation in domed peatlands, our analysis also revealed peatlands (domed and not domed), independent of latitude or climate characteristics, without such a correlation (Figures 5c, 5d, and 5h; see also Table S1 of the Supporting Information). This absence of correlation occurs over a variety of peatland types (Figures S1d–S1f of the Supporting Information show three schematics). One common case is a mire with a flat surface and concave bottom, as described by Lähteenoja and Page (2011) for a site in Peru (Figure 5h). We can see from the plot that the surface elevation is almost constant along the transect, while the peat thickness varies from 0 to ~5 m. Flat surface mires with concave bottoms and low correlation coefficients were also found by Silvestri et al. (2019) in Norway (Figure 5c – orange squares). In these cases, given that the surface elevation is the same across the mire, it cannot be used for predicting the peat thickness.

Another common category is domed mires with irregular bottom surfaces, as in the cases studied in Indonesia by Esterle and Ferm (1994) (Figure 5d). Kowalczyk et al. (2017) describes the case of a mire with almost flat surface and irregular bottom in Poland (Figure 5c – purple diamonds). In these cases, the peat thickness varies independently from the surface elevation, as seen in the lack of correlation between the elevations of the top and bottom surfaces reported in Figure S1d of the Supporting Information.

A different situation is described by Dargie et al. (2017) in a study of a very large mire in Congo. In this case, Figure 5f shows a clear lack of correlation between peat thickness and surface elevation due to the irregular shape of both the top and the bottom of the peatland.

Based on these findings, we develop a simplified framework for describing the topographic relationships between the peat surface and bottom elevations that we can find in nature. We represent the mire as a flattened spheroid (in agreement with the semielliptical surface profile described by Ingram, 1982). To simulate the acquisition of measurements along a transect in the field, we consider a vertical plane through the peat body producing a 2-D interception. A more detailed geometric description of the model and a simple mathematical explanation is included in the Supporting Information.

Shown in Figure 6 are schematics of the cases considered, varying the shapes of the bottom surface of a mire and keeping the top unchanged. Our first case, convex-concave, always results in the slope *m* (i.e., ratio between peat thickness and soil elevation) being greater than 1. If we have a perfectly specular shape of the peat body with respect to the horizontal plane, the slope is equal to 2. When the elevation of the bottom of the peat decreases faster than the increase of the top surface, the slope is greater than 2. When we have the opposite case, the slope is less than 2.

When the mire bottom is flat, the slope of the regression line between soil elevation and peat thickness equals 1 as shown in Figure 6. In this case, referred to as convex-flat mires, the change in elevation is equivalent to the change in peat thickness. When we have a convex-convex profile, i.e., both the top and the bottom of the mire are convex, the slope of the regression line is less than 1. The chosen framework for the empirical approach shows that, when there is a linear correlation between peat topography and bottom shape, *m* can be used to categorize different morphological types of peatlands, because the difference in the slope is dictated by the difference of the curvature in the surface profile with respect to the curvature of the peat bottom profile. The mathematical explanation included in the Supporting Information shows that the chosen

framework for the empirical approach is not unique; other peat profiles, regardless of the shape of the domed mire, may be characterized by the covariation of the peatland bottom and surface and consequently by the existence of the linear correlation between peat thickness and surface elevation. This covariation is not a special case; on the contrary, it is likely to be common for domed mires across the world as illustrated in Figure 5 for peatlands situated on different continents and at different latitudes. The convex-concave peatlands have likely developed over depressed terrain that allowed the accumulation of peat starting in the center of the depression, as confirmed by dating analyses of samples collected in several studies (Richardson, 2008; Rydin & Jeglum, 2013). Once the depression is concentrically filled with organic soil, the hydrological conditions favor the development of a domed bog, which is a common situation in both high-latitude (Gorham, 1957; Rydin & Jeglum, 2013) and tropical (Craft & Richardson, 1998; Householder et al., 2012) environments. However, peat also accumulates over flat lands, as confirmed by the convex-flat profile. Importantly, our findings are consistent with peatland studies where the lowest subsurface areas on the landscape result in the production of the thickest peat domes while shallower peats are found on subsurface mineral ridges (Glaser et al., 1997; Rydin & Jeglum, 2013).

We have now explained why and in what specific cases a correlation between peat thickness and surface elevation exists (Research Question 1). We must now determine (2) to what extent this correlation is transferable across locations. In order to answer our second question, we use as an example the study performed by Cameron and Schruben (1983) for a peatland area in Maine; this study is commented on in Supporting Information (see Figure S4). As seen in other studies, Cameron and Schruben (1983) reported observations on a series of closely-spaced individual mires. Since each mire has a specific and unique correlation between the surface and the bottom shape, we show that when observations performed on one mire are used to infer the thicknesses of other nearby mires, significant errors are incurred. In this situation, the determination of the boundary of each mire is essential in order to establish any possible correlation between peat thickness and elevation. However, such determination may not be easy to establish a priori, leading to overestimation or underestimation of the actual peat volume. It is also important to note that without sufficient a priori knowledge of the study site, it would be impossible to determine the correct number and distribution of ground-based sampling locations needed to determine the correlation (i.e., the correct m) that would make it possible to calculate peat thickness from a measurement of surface elevation. This is particularly true for large study sites containing several mires. The transferability of a specific correlation between peat thickness and surface elevation found for a certain mire may also be affected by the effects of peat degradation. It should, in fact, be recognized that our analysis refers to peatlands in undisturbed conditions. Disturbance due to draining, burning, and flattening of the peatland surface may result in changes to the relation between thickness and elevation, resulting in a modified correlation slope, m (or even the absence of any correlation). Thus, even if we recognize that the slope may provide information on disturbance level and history, it may also lead to an erroneous estimation of the peat volume for one mire and hence for the nearby mires if this correlation is transferred. Collectively, our analyses show that the correlation between peat thickness and surface elevation is site-dependent and may provide erroneous peat volume estimates once it is extended to other sites or to large territories.

At our study site, the linear correlation between peat thickness and soil topography is visible in Figures 7a and 7b, where we divide the 63 coring sites into two groups, with 14 in the West dome (Figure 7a) and 49 in the East dome (Figure 7b). In order to broadly characterize the morphology of the two peatlands, we start with analyzing the measurements collected in the field. If we examine the correlation between peat thickness and surface elevation for the two peatlands separately (Figures 7a and 7b), we find two different slopes. While for the West peatland the linear correlation is very poor ($R^2 = 0.17$), peat thickness is strongly correlated with surface elevation for the East mire ($R^2 = 0.82$). In this case, the slope $m = 0.94$ indicating that the peat bottom tends to be flat. However, if the area is treated as one peatland and all the available measurements are plotted together, m of 0.74 is obtained ($R^2 = 0.73$) (not shown in the figure for brevity), leading to the erroneous conclusion that the bottom of the peatland is convex for the entire area. Using this correlation, with $m = 0.74$, over the entire site would result in an underestimation of peat thickness in areas of the East dome with thick peat and produce unreliable thickness estimates for the West dome where, in fact, the correlation between thickness and surface elevation is weak.

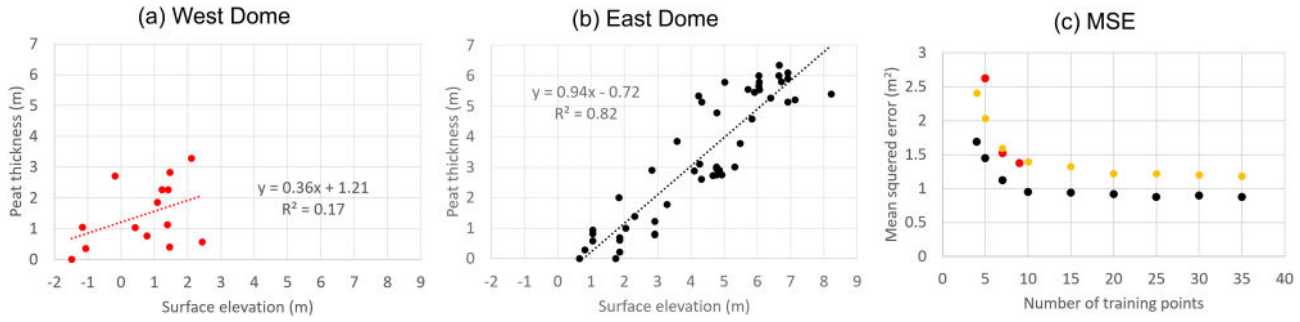

Figure 7. Linear regression models for the (a) West and the (b) East domes of the study site. (c) Mean squared error (MSE) of the empirical model calculated using a variant of the K-fold cross validation randomly dividing the data into a test and a training set. The MSE is the average squared error across all trials. For the West mire (red dots): test set (for validation) = 5 points; training set (for calibration) = 5, 7, and 9 points; number of trials: 30. For the East mire (black dots): test set (for validation) = 14 points; training set (for calibration) = 4, 5, 7, 10, 15, 20, 25, 30, and 35 points; number of trials: 100. Considering the whole dataset of 63 field measurements (yellow dots): test set (for validation) = 14 points; training set (for calibration) = 4, 5, 7, 10, 15, 20, 25, 30, and 35 points; number of trials: 250.

In order to explore the accuracy of the empirical approach, we consider three scenarios. The first (ideal) case is one in which a detailed description of the morphology of the study site is available and we know a priori that there are two contiguous but distinct mires and their exact boundaries. In this scenario, we perform a cross validation of the empirical method results obtained when two regression lines were calculated separately for the West and the East mire. Specifically, in order to assess the error, we randomly pick a number of the field points (5 for the West mire and 14 for the East mire) using them as the testing sample set and use the remaining measurements as the training sample set to fit the empirical linear correlation. This process is repeated several times with different combinations and allows us to calculate the error in predicting peat thickness from the empirical method. Figure 7c shows that in general, the MSE of the empirical method decreases when the number of measurements that are used during the training phase increases but quickly reaches a point where, even if the number of measurements increases, the MSE stays stable. This is the case of the East dome, for which the MSE stays stable at around 0.9 m^2 as the number of measurements equals or exceeds 10. The same behavior is noticed when the entire dataset is used: in this case the MSE, is constantly higher and stays stable at around 1.2 m^2 as the number of measurements equals or exceeds 20. The error is consistently higher for the West dome than for the East dome also because the number of field measurements used for training is lower than 10 (MSE larger than 1.3 m^2).

In a second scenario, no a priori detailed information is available about the study site, and we use all the field measurements together, fitting one single empirical line to predict the peat thickness across both mires. In this case (Figure 7c), the MSE is consistently higher than the one calculated for the East dome and similar to the one calculated for the West dome. The MSE is higher than 1.3 m^2 if the number of field measurements is equal to or smaller than 15, and it is around 1.2 m^2 if the available measurements exceed 20 points. We speculate that this is the most likely scenario; as when a survey is planned in a new area, there is often limited a priori information available.

The third scenario describes the case of using the measurements performed in one of the two peatlands to determine the empirical linear correlation and use it to predict the peat thickness of the second peatland. In this scenario, if we use the empirical model calculated for the West dome to predict the thickness of the East dome, the MSE is 2.4 m^2. If we use the empirical model calculated for the East dome to predict the thickness of the West dome, the MSE increases to 3.6 m^2. These results confirm that the empirical method cannot be reliably transferred across peatlands.

3.4. Comparison of the Airborne Electromagnetic Method with the Empirical Topographic Approach

In order to compare the results obtained with the AEM method with those obtained with the empirical approach, in Figure 8, we consider several selected AEM transects that intercept the locations of the field measurements (i.e., only AEM transects that fall less than 20 m from the field measurement points were selected).

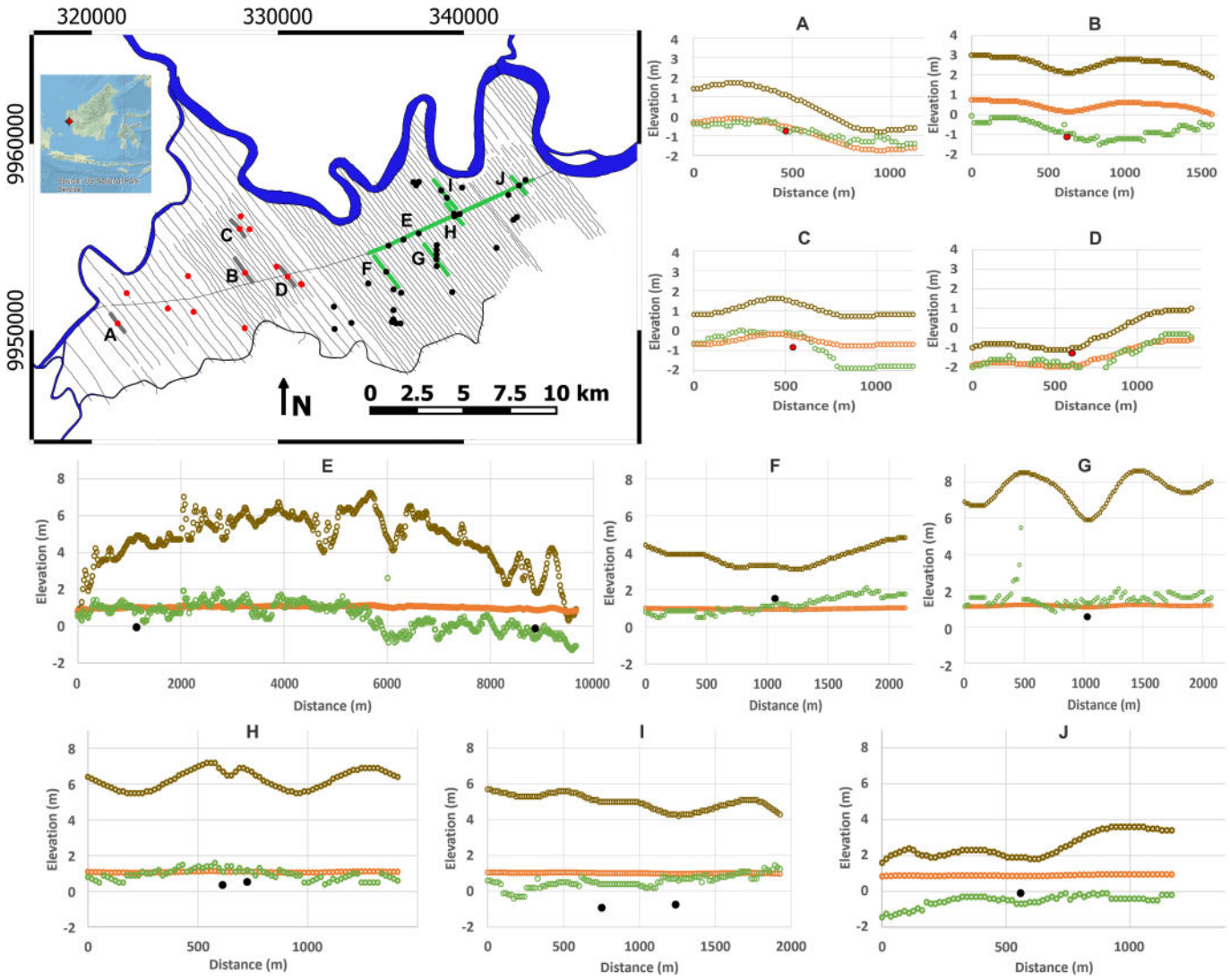

Figure 8. Map of the SkyTEM flight lines over the study site. Red and black dots correspond to the coring locations in the West and East peatlands respectively (Coordinate reference system: WGS84 UTM 49S). Transects report the comparisons between the bottom elevation simulated using the empirical approach (orange dots) and the bottom elevation retrieved from the AEM data (green dots) along the transects visible in the map. Brown dots define the surface topography measured using the laser altimeters carried by the SkyTEM system, while red and black dots correspond to the field measurements located less than 20 m from the nearest AEM measurement.

Also shown in Figure 8 are the bottom profiles of the peat predicted along the transects from surface elevation using the empirical model calculated for the West and the East domes separately. The profiles mapped with the AEM method show significant variability in the shape of the bottom surface of the peat, which is possibly due to the high spatial variability of the peat bottom at the local scale as observed by the triplets of measurements performed in the field (see Figure S5). In general, we note that the field core measurements agree with the AEM profiles. The agreement is particularly evident where the peat thickness is intermediate, i.e., between 2 m and 5 m (transects B, E, and J), and in these cases, the mapping of the bottom elevation using the AEM method is more accurate than using the empirical approach. Along transect D, the peat is very shallow (less than 1 m), and both the AEM method and the empirical approach tend to overestimate the thickness, while along transect H the thicknesses are larger than 5 m, and both tend to underestimate them but to varying degrees.

The consistent difference found between the peat thickness prediction abilities of the two methods propagates into the calculation of the total peat volume. Specifically, using the empirical approach separately

for the two mires (i.e., the most favorable scenario), we calculate a peat volume of almost 410 million cubic meters (409,235,293 m^3), while the volume calculated using AEM data is 22% higher, about 500 million cubic meters (499,879,707 m^3). Given the average organic carbon content by soil volume of 0.054 g/cm^3 retrieved from the laboratory analysis, we calculate that this peatland stores 22.1 Mt of organic carbon if we consider the volume given by the empirical method. Considering the volume retrieved with the AEM method, we have a much larger content of organic carbon, equal to 27 Mt. This is due to the intrinsic lack of capability that the empirical approach has to follow the changes of thickness (e.g., of peat bottom elevation) at the local scale, changes that are confirmed by our closely-spaced coring measurements (Figure S5). This appears to produce a general underestimation of the peatland volume using the linear model, with important consequences for the quantification of the carbon stored in the system. The high density of AEM data, on the contrary, allows for the description of the bottom morphology at a high spatial resolution, detecting changes over small distances.

4. Discussion

The morphology of peatlands, especially those with a domed surface, has long fascinated ecologists, geomorphologists, and geologists. Historically, there have been studies seeking to understand how the surface morphology of domed mires (i.e., peatland dominated by living peat-forming plants that have a raised surface with respect to the surrounding lands) develop and the dependence of peat formation on hydrological variables, i.e., rainfall and drainage patterns (Ingram, 1982; Clymo, 1984; Foster & Wright, 1990; Belyea & Baird, 2006; Cobb et al., 2017). The topographic shape and patterns within peatlands reflect the interactions between underlying terrain form, climate, and hydrology, i.e., hydromorphology (Cobb et al., 2017; Rydin & Jeglum, 2013). However, past efforts were devoted to the characterization of the surface profile of peatlands, i.e., its topography, ignoring the importance of studying the profile of the peat bottom, which is set as a horizontal surface boundary condition in both Ingram's and Clymo's peat growth models.

The geophysical approach based on the AEM method allowed us, for the first time, to map out at high spatial resolution the variation in the elevation of the peatland surface and the peatland base, revealing the peatland top and bottom morphology and allowing for the accurate quantification of peat volume. The level of contrast between the resistivity of the peat and that of the underlying clay substrate, typical of Indonesian peatlands and many others worldwide, provided the conditions required for the application of the AEM method. The great advantage of the AEM method, relative to other ground-based geophysical methods, is the speed of data acquisition, allowing for fast detection of the interface over large distances. The absence of interference due to the presence of infrastructure and power lines, which is a typical limitation for AEM applications in regions with high population density, further facilitated the application of the methodology. We conclude that in similar conditions the AEM approach can provide the critical information needed to quantify peat volume and carbon storage from the local to the landscape scale.

The AEM method applied in this study has the great advantage of imaging the shape of the peat top and bottom virtually instantaneously, as the helicopter takes just a few days to cover large territories. This allows the assessment of the peat volume and carbon content even on lands that undergo degradation effects, which usually result in the loss of peat mass and consequent subsidence of the soil surface. Ideally, the repetition of AEM surveys over degrading peatlands would make it possible to follow the loss of mass and to eventually assess the amount of carbon dioxide emitted due to this process. A similar approach has been shown very effective by Ballhorn et al. (2009) using LiDAR data collected before and after fires. However, since the AEM images both the top and the bottom of the peat, the method can be used to follow the evolution of the entire 3-D peat body.

The main limitations that we have noticed in the application of the AEM to the study site are (1) the difficulty in detecting a sharp transition between the peat and the substrate, and (2) the decreased accuracy obtained in retrieving the peat thickness between flight lines. In situations where there is a limited resistivity contrast between the peat and substrate, or a gradual transition between the two, it is more challenging to detect the base of the peat; these two factors likely varied throughout the study site. As for the increased error in peat thickness assessment between flight lines, we believe it is due to the large spatial variability of the peat thickness. The spatial sampling of the subsurface with the AEM method needs to be sufficient to capture the spatial variability; the shorter the distance over which peat thickness varies, the closer the flight

lines need to be to accurately capture the variation in thickness. There will always be a trade-off between the increased accuracy achieved with closer line spacing and the increased cost of acquiring more data. More work is needed in order to understand how the use of ancillary data and/or the production of a well-characterized covariance model may be used to optimize data acquisition. Another potential limitation, in other locations, is when peat soils are sitting on top of more resistive material (i.e., a sandy mineral-soil matrix), which is a common situation in coastal sites in Indonesia (i.e., related to colonization of swamps over sandy ridges). The use of AEM for peat volume mapping over resistive substrate has been recently found to be effective in boreal peatlands (Silvestri et al., 2019); however, further studies are needed in order to extend the application of this method to tropical peatlands.

Our results show that a linear correlation between peat thickness and peatland topography is common in some dome-shaped peatlands across the world. Exploring a number of topo-stratigraphic profiles extracted from several studies, we were able to categorize, from a morphological prospective, the combinations of surface and bottom shapes that make such linearity possible. The linearity of the relationship between peat thickness and surface elevation implies that, along measuring transects, the bottom profile of the peat mires covaries with the topography, i.e., when the surface elevation increases, the bottom elevation either increases or decreases accordingly. Even though these findings provide new insights on the morphological characteristics of peatlands, we show that the empirical model based on the linear correlation between peat thickness and peatland surface elevation has limited prediction capabilities. In fact, as with many other empirical models, its accuracy strongly depends on the number and spatial coverage of available field observations to calibrate the model. Moreover, since the linear correlation is site-specific, the empirical model provides erroneous peat volume estimates once it is extended to other sites or to large territories.

Our application to a real case study shows that the empirical approach linearly linking peat thickness to surface elevation may provide a simple conceptual model of the peatland morphology as long as detailed a priori information is available. Unless the morphology of the two peatlands present in the study site is well known a priori, the error associated with the empirical approach in predicting the peat thickness is high. As an example, we note that the weak correlation between peat thickness and topography characterizing the West peatland may be due to the advanced state of peat degradation resulting from reclamation efforts, which probably produced land subsidence. Different zones of the peatland were reclaimed in different periods, starting in the 1980s, resulting in uneven subsidence of the area, which in turn affected the original correlation between peat thickness and topography. The East peatland has been reclaimed only recently, and thus, the degradation process has only recently started to impact its surface topography. We thus conclude that the use of the empirical approach for peat thickness quantification is risky and should be used only to obtain an approximate description of the peatland morphology. Furthermore, we note that the Indonesian site selected for this study does not reveal how uncertain the prediction produced with the empirical model may become. At this site, the two peatlands are similar, both showing peat thicknesses between 0 and 7 m, and the bottom is almost flat, especially for the East dome. In general, whenever the peat thickness range differs between two peatlands, the error in predicting the thickness using mixed data or data extrapolated only from one of the two peatlands increases considerably. On the contrary, the high spatial resolution of the thickness retrievals from AEM data guarantees high accuracies, especially along the flight lines, regardless of the morphology of the peatland.

5. Conclusions

Our results show that the AEM method can detect both the top and the bottom of a peatland profile over large areas at high spatial resolution, allowing for a comprehensive three-dimensional morphological description of the peat body that yields accurate estimates of peat thickness at large (i.e., km) scales of measurement. This method can be used to quantify the total peat volume, regardless of the surface topography of the peatland. In this study, we deliberately avoided the use of field measurements to constrain the data inversion, in order to allow the assessment of this technique per se. However, limited coring data may initially be needed to assist with identifying the transition between the peat and the underlying substrate, as the changing electrical properties in the transition zone may produce uncertainties in the detection of a precise boundary. Properly employed, the AEM methodology is robust and accurate. In our study, we show that it performs extremely well along the flight lines, where the instrument clearly detects the peat layer and

differentiates it from the underlying mineral substrate. Moving away from the flight lines, the highly variable structure of the peat is more difficult to capture in the interpolation of the AEM data but is still more accurate than using the empirical approach. In varying dome conditions, a higher flight line density is preferable to describe the spatial distribution of the peat layer. The main issue with this technology is the perception of its high cost; but the saving in terms of time to map peat thickness throughout large areas is enormous when compared to other methods. Another potential limitation in the applicability of the AEM method (although not an issue at our study site) is the presence of infrastructure that interferes with the signal. Finally, in the case of highly variable carbon content within the peat body, the AEM method may not provide adequate resolution (vertical and horizontal) to accurately detect the corresponding variability in the electrical resistivity, meaning some field testing and analysis a priori are recommended.

In this study, we have also explored the feasibility of predicting the peat thickness based on its apparent correlation to the soil topography. Our analysis of several previous studies available from the literature has shown that a linear correlation is present only in some dome-shaped peatlands. We could not find any specific characteristic of the peatland (e.g., latitude, climate, vegetation cover type, etc.) that makes it possible to determine if such a correlation is present a priori. In those cases, where a correlation does exist, the geographic area over which it is valid can be very limited; the correlation can vary between individual mires. When used for predicting the peat thickness, the empirical topographic model can broadly describe the morphological characteristics of a peatland and can be used to calculate its peat volume only when the linear correlation between peat thickness and surface elevation is strong. In such cases, the prediction accuracy strongly depends on the number and specific locations of available field observations, and in case of degraded/reclaimed systems, on the grade and homogeneity of the degradation across the peatland. Since the linear correlation is site-specific, it provides incorrect peat volume estimates when it is extended to other sites or over large territories. When compared to the AEM method, our results show that the AEM method is superior in detecting the peat morphology and volume.

Conflict of Interest

The authors declare the following competing interest: Andrea Viezzoli is the head of a small company that provides technical support for the analysis of AEM data.

Data Availability Statement

Field/lab data and analyses results are available at doi: 10.5281/zenodo.3572061, and Airborne Electromagnetic (AEM) data are available at doi: 10.5281/zenodo.3571918.

Acknowledgments
SkyTEM data acquisition was funded by David and Lucile Packard Foundation through the Grant 2017-65823 to Duke University. Field activities and the acquisition of some additional SkyTEM data were supported by Stanford University School of Earth, Energy and Environmental Sciences, the Duke Wetland Center, SkyTEM Geophysical Surveys, and EnviroSolutions & Consulting. This research is part of the project CReScenDo (Combining Remote Sensing Technologies for Peatland Detection and Characterization) that has received funding from the European Union's Horizon 2020 research and innovation program under the Marie Skłodowska-Curie Grant 747809. We wish to thank Andy Parsekian and Ahmad Behroozmand for helpful discussions in the planning of the data acquisition and their preliminary analysis. We also thank the SkyTEM team and the company director Flemming Effersø who provided their experience and support during the survey.

References

Aarhus GeoSoftware (2018). Aarhus Workbench. Available online at: https://www.aarhusgeosoftware.dk/

Anshari, G. Z., Afifudin, M., Nuriman, M., Gusmayanti, E., Arianie, L., Susana, R., et al. (2010). Drainage and land use impacts on changes in selected peat properties and peat degradation in West Kalimantan Province, Indonesia. *Biogeosciences*, *7*(11), 3403–3419.

Auken, E., & Christiansen, A. V. 2004. Layered and laterally constrained 2D inversion of resistivity data. *Geophysics*, *69*(3),752–761

Ballhorn, U., Jubanski, J., & Siegert, F. (2011). ICESat/GLAS data as a measurement tool for peatland topography and peat swamp forest biomass in Kalimantan, Indonesia. *Remote Sensing*, *3*, 1957–1982.

Ballhorn, U., Siegert, F., Mason, M., & Limin, S. (2009). Derivation of burn scar depths and estimation of carbon emissions with LIDAR in Indonesian peatlands. *Proceedings of the National Academy of Sciences*, *106*(50), 21,213–21,218. https://doi.org/10.1073/pnas.0906457106

Belyea, L. R., & Baird, A. J. (2006). Beyond "the limits to peat bog growth": Cross-scale feedback in peatland development. *Ecological Monographs*, *76*(3), 299–322.

Clymo, R. S. (1984). The limits to peat bog growth. *Philosophical Transactions of the Royal Society of London. B, Biological Sciences*, *303*(1117), 605–654.

Cameron, C. C., & Schruben, P. 1983. *Variations in mineral-matter content of a peat depositresting on glacio-marine sediments in Maine*. In R. Raymond & M. J. Andrejko (Eds.), *Mineral Matter in Peat, its Occurrence, Form, and Distribution* (pp. 63–76). Los Alamos National Laboratory, Los Alamos, NM.

Cobb, A. R., Hoyt, A. M., Gandois, L., Eri, J., Dommain, R., Salim, K. A., et al. (2017). How temporal patterns in rainfall determine the geomorphology and carbon fluxes of tropical peatlands. *Proceedings of the National Academy of Sciences*, *114*(26), E5187–E5196.

Comas, X., Terry, N., Hribljan, J. A., Lilleskov, E. A., Suarez, E., Chimner, R. A., & Kolka, R. K. (2017). Estimating belowground carbon stocks in peatlands of the Ecuadorian páramo using ground-penetrating radar (GPR). *Journal of Geophysical Research: Biogeosciences*, *122*, 370–386.

Comas, X., Terry, N., Slater, L., Warren, M., Kolka, R., Kristiyono, A., et al. (2015). Imaging tropical peatlands in Indonesia using ground-penetrating radar (GPR) and electrical resistivity imaging (ERI): Implications for carbon stock estimates and peat soil characterization. *Biogeosciences*, *12*, 2995–3007. https://doi.org/10.5194/bg-12-2995-2015

Craft, C. B., & Richardson, C. J. (1998). Recent (137Cs), long-term (210Pb) and historical (14C) peat accretion and nutrient accumulation in Everglades peatlands. *Soil Science Society of America Journal*, *62*, 834–843.
Cubizolle, H., Bonnel, P., Oberlin, C., Tourman, A., & Porteret, J. (2007). Advantages and limits of radiocarbon dating applied to peat inception during the end of the Lateglacial and the Holocene: The example of mires in the Eastern Massif Central (France). *Quaternaire. Revue de l'Association française pour l'étude du Quaternaire*, *18*(2), 187–208.
Dargie, G. C., Lewis, S. L., Lawson, I. T., Mitchard, E. T. A., Page, S. E., Bocko, Y. E., & Ifo, S. A. (2017). Age, extent and carbon storage of the Central Congo Basin peatland complex. *Nature*. https://doi.org/10.1038/nature21048
DeLaune, R. D., Reddy, K. R., Richardson, C. J., & Megonigal, J. P. (Eds) (2013). *Methods in biogeochemistry of wetlands*, *Soil Science Society of America Book Series No* (Vol. 10). Soil Science Society of America: Madison, WI.
Deltares (2016). Exploration of the use of LiDAR data in peatland mapping and management in Indonesia – Status update April 2016 - https://www.deltares.nl/app/uploads/2015/03/Overview-LiDAR-use-in-peat-management-Indonesia-Deltares-April-2016.pdf (downloaded on March 2019).
Draper, F. C., Roucoux, K. H., Lawson, I. T., Mitchard, E. T., Coronado, E. N. H., Lähteenoja, O., et al. (2014). The distribution and amount of carbon in the largest peatland complex in Amazonia. *Environmental Research Letters*, *9*(12), p.124017.
Esterle, J. S., & Ferm, J. C. (1994). Spatial variability in modern tropical peat deposits from Sarawak, Malaysia and Sumatra, Indonesia: analogues for coal. *International Journal of Coal Geology*, *26*(1-2), 1–41.
FAO (1988). Soil map of the world, revised legend. World Soil Resources Report 60, Food and Agriculture Organization of the United Nations, Rome.
FAO (1998). World reference base for soil resources, Food and Agriculture Organization of the United Nations, International Soil Reference and Information Centre and International Society of Soil Science, Rome.
Foster, D. R., Wright Jr., H. E. (1990). Role of ecosystem development and climate change in bog formation in central Sweden. *Ecology*, *71*(2), 450–463.
Glaser, P., Siegel, H., Romanowicz, D. I., Ping, E. A., & Shen, Y. (1997). Regional linkages between raised bogs and the climate, groundwater, and landscape of north-western Minnesota. *Journal of Ecology*, *85*, 3–16.
Gorham, E. (1957). The development of peatlands. *Quarterly Review of Biology*, *32*, 145–166.
Gorham, E. (1991). Northern peatlands: Role in the carbon cycle and probable responses to climatic warming. *Ecological Applications*, *1*(2), 182–195. https://doi.org/10.2307/1941811
Holden, N. M., & Connolly, J. (2011). Estimating the carbon stock of a blanket peat region using a peat depth inference model. *Catena*, *86*(2), 75–85.
Hooijer, A. and Vernimmen, R. (2013). Peatland maps for Indonesia. Including accuracy assessment and recommendations for improvement, elevation mapping, and evaluation of future flood risk. Quick Assessment and Nationwide Screening (QANS) of Peat and Lowland Resources and Action Planning for the Implementation of a National Lowland Strategy – PVW3A10002. Agentschap NL 6201068 QANS Lowland Development, for Government of Indonesia and Partners for Water (DELTARES, Netherlands) - https://www.deltares.nl/app/uploads/2015/03/QANS-Peat-mapping-report-final-with-cover.pdf (downloaded on March 2019).
Householder, J. E., Janovec, J. P., Tobler, M. W., Page, S., & Lähteenoja, O. (2012). Peatlands of the Madre de Dios River of Peru: Distribution, geomorphology, and habitat diversity. *Wetlands*, *32*(2), 359–368.
Høyer, A. S., Jørgensen, F., Sandersen, P. B. E., Viezzoli, A., & Møller, I. (2015). 3D geological modelling of a complex buried-valley network delineated from borehole and AEM data. *Journal of Applied Geophysics*, *122*, 94–102. https://doi.org/10.1016/j.jappgeo.2015.09.004
Ingram, H. A. P. (1982). Size and shape in raised mire ecosystems: A geophysical model. *Nature*, *297*, 300–303.
Jaenicke, J., Rieley, J. O., Mott, C., Kimman, P., & Siegert, F. (2008). Determination of the amount of carbon stored in Indonesian peatlands. *Geoderma*, *147*(3–4), 151–158.
Joosten, H., Moen, A., & Couwenberg, F. T. (2017). Mire diversity in Europe: Mire and peatland types. In H. Joosten, F. Tanneberger, & A. Moen (Eds.), *Mires and peatlands of Europe: Status, distribution and conservation* (Chap. 2, pp. 5–64). Stuttgart Germany: Schweizerbart Science Publishers.
Kirkegaard, C., & Auken, E. (2014). A parallel, scalable and memory efficient inversion code for very large scale airborne EM surveys. *Geophysical Prospecting*, *63*, 495–507.
Knight, R., Smith, R., Asch, T., Abraham, J., Cannia, J., Viezzoli, A., & Fogg, G. (2018). Mapping aquifer systems with airborne electromagnetics in the central valley of California. *Groundwater*, *56*(6), 893–908. https://doi.org/10.1111/gwat.12656
Könönen, M., Jauhiainen, J., Laiho, R., Kusin, K., & Vasander, H. (2015). Physical and chemical properties of tropical peat under stabilised land uses. *Mires and Peat*, *16*(8), 1–13.
Kowalczyk, S., Żukowska, K. A., Mendecki, M. J., & Łukasiak, D. (2017). Application of electrical resistivity imaging (ERI) for the assessment of peat properties: A case study of the Całowanie Fen, Central Poland. *Acta Geophysica*, *65*(1), 223–235.
Lähteenoja, O., & Page, S. (2011). High diversity of tropical peatland ecosystem types in the Pastaza-Marañón basin, Peruvian Amazonia. *Journal of Geophysical Research*, *116*, G02025. https://doi.org/10.1029/2010JG001508
McClellan, M., Comas, X., Benscoter, B., Hinkle, R., Sumner, D. (2017). Estimating belowground carbon stocks in isolated wetlands of the Northern Everglades Watershed, central Florida using ground penetrating radar (GPR) and aerial imagery. *Journal of Geophysical Research: Biogeosciences*, *122*, 2804–2816. https://doi.org/10.1002/2016JG003573
Miettinen, J., Shi, C., Tan, W., & Liew, S. (2012). 2010 land cover map of insular Southeast Asia in 250-m spatial resolution. *Remote Sensing Letters*, *3*(1), 11–20.
Page, S. E., Rieley, J. O., Shotyk, Ø. W., & Weiss, D. (1999). Interdependence of peat and vegetation in a tropical peat swamp forest. *Philosophical Transactions of the Royal Society of London B: Biological Sciences*, *354*(1391), 1885–1897. https://doi.org/10.1098/rstb.1999.0529
Page, S. E., Siegert, F., Rieley, J. O., Boehm, H. D. V., Jaya, A., & Limin, S. (2002). The amount of carbon released from peat and forest fires in Indonesia during 1997. *Nature*, *420*(6911), 61.
Parry, L. E., Charman, D. J., & Noades, J. P. W. (2012). A method for modelling peat depth in blanket peatlands. *Soil Use and Management*, *28*(4), 614–624.
Parry, L. E., West, L. J., Holden, J., & Chapman, P. J. (2014). Evaluating approaches for estimating peat depth. *Journal of Geophysical Research: Biogeosciences*, *119*, 567–576. https://doi.org/10.1002/2013JG002411
Parsekian, A. D., Comas, X., Slater, L., Glaser, P. H. (2011). Geophysical evidence for the lateral distribution of free phase gas at the peat basin scale in a large northern peatland. *Journal of Geophysical Research*, *116*, G03008. https://doi.org/10.1029/2010JG001543
Podgorski, J. E., Auken, E., Schamper, C., Vest Christiansen, A., Kalscheuer, T., & Green, A. G. (2013). Processing and inversion of commercial helicopter time-domain electromagnetic data for environmental assessments and geologic and hydrologic mapping. *Geophysics*, *78*(4), E149–E159. https://doi.org/10.1190/geo2012-0452.1

Richardson, C. J. (2008). *The Everglades experiments: Lessons for ecosystem restoration* (p. 698). New York: Springer-Verlag.
Rydin, H., & Jeglum, J. K. (2013). *The biology of peatlands*, (2nd (ed) ed.). Oxford: Oxford University Press.
Rudiyanto, Setiawan, B. I., Arief, C., Saptomo, S. K., Gunawan, A., Kuswarman, Sungkono, Indriyanto, A. (2015). Estimating Distribution of Carbon Stock in Tropical Peatland Using a Combination of an Empirical Peat Depth Model and GIS. *Procedia Environmental Sciences*, *24*, 152–157. https://doi.org/10.1016/j.proenv.2015.03.020
Sattel, D., & Kgotlhang, L. (2004). Groundwater exploration with AEM in the Boteti area, Botswana. *Exploration Geophysics*, *35*(2), 147–156.
Schamper, C., Jørgensen, F., Auken, E., & Effersø, F. (2014). Assessment of near-surface mapping capabilities by airborne transient electromagnetic data – An extensive comparison to conventional borehole data. *Geophysics*, *79*(4), B187–B199.
Scharlemann, J. P., Tanner, E. V., Hiederer, R., & Kapos, V. (2014). Global soil carbon: Understanding and managing the largest terrestrial carbon pool. *Carbon Management*, *5*(1), 81–91.
Silvestri, S., Christensen, C. W., Lysdahl, A. O. K., Anschütz, H., Pfaffhuber, A. A., & Viezzoli, A. (2019). Peatland volume mapping over resistive substrates with airborne electromagnetic technology. *Geophysical Research Letters*, *46*, 6459–6468. https://doi.org/10.1029/2019GL083025
Slater, L. D., & Reeve, A. (2002). Investigating peatland stratigraphy and hydrogeology using integrated electrical geophysics. *Geophysics*, *67*(2), 365–378.
Soil Survey Staff (2014a). *Keys to soil taxonomy*, (12th ed.). Washington, DC: USDA-Natural Resources Conservation Service.
Soil Survey Staff (2014b). Soil survey field and laboratory methods. Soil Survey Investigations Report No. 51, Version 2.0. R. Burt and Soil. Survey Staff (ed.). U.S. Department of Agriculture, Natural Resources. Conservation Service.
Sørensen, K. I., & Auken, E. (2004). SkyTEM – A new high-resolution helicopter transient electromagnetic system. *Exploration Geophysics*, *35*(3), 191–199.
Supardi, S. A. D., & Neuzil, S. G. (1993). General geology and peat resources of the Siak Kanan and Bengkalis Island peat deposits, Sumatra, Indonesia. In J. C. Cobb, & C. B. Cecil (Eds.), *Modern and Ancient Coal-Forming Environments*, *Special Paper* (Vol. 286, pp. 45–61). Boulder, Colorado: Geological Society of America.
Turetsky, M. R., Benscoter, B., Page, S., Rein, G., Van der Werf, G. R., & Watts, A. (2015). Global vulnerability of peatlands to fire and carbon loss. *Nature Geoscience*, *8*(1), 11.
Viezzoli, A., Christiansen, A. V., Auken, E., & Sørensen, K. I. (2008). Quasi-3D modeling of airborne TEM data by Spatially Constrained Inversion. *Geophysics*, *73*, 3, F105–F113
Von Post, L. & Granlund, E. (1926). Peat resources in southern Sweden – Sveriges geologiska undersökning, Yearbook.
Warner, B. G., Nobes, D. C., & Theimer, B. D. (1990). An application of ground penetrating radar to peat stratigraphy of Ellice Swamp, southwestern Ontario. *Canadian Journal of Earth Sciences*, *27*(7), 932–938. https://doi.org/10.1139/e90-096
Warren, M., Hergoualc'h, K., Kauffman, J. B., Murdiyarso, D., & Kolka, R. (2017). An appraisal of Indonesia's immense peat carbon stock using national peatland maps: uncertainties and potential losses from conversion. *Carbon Balance and Management*, *12*(1), 12.
Yu, Z., Loisel, J., Brosseau, D. P., Beilman, D. W., & Hunt, S. J. (2010). Global peatland dynamics since the Last Glacial Maximum. *Geophysical Research Letters*, *37*, L13402. https://doi.org/10.1029/2010GL043584